Clays and Clay Minerals, Vol. 53, No. 5, 466–477, 2005.

CHLORITE IN METABASITES FROM THE MIKABU AND NORTH CHICHIBU BELTS, SOUTHWEST JAPAN

MASAAKI MIYAHARA[1,3], RYUJI KITAGAWA[1] AND SEIICHIRO UEHARA[2]

[1] Graduate School of Science, Hiroshima University, 1-3-1 Kagamiyama, Higashi-Hiroshima, Hiroshima, 739-8526, Japan
[2] Department of Earth and Planetary Sciences, Faculty of Science, 33, Kyushu University, Hakozaki, 6-10-1, Fukuoka, 812-8581, Japan
[3] Graduate School of Science, Tohoku University, 6-3 Aramaki Aoba-ku Sendai, Miyagi, 980-8578, Japan

Abstract—Chlorites formed as a replacement of phenocrysts in metabasites from the pumpellyite-actinolite to lower-greenschist facies Mikabu and North Chichibu belts in southwest Japan were studied by X-ray powder diffraction, electron microprobe analysis (EMPA) and high-resolution transmission electron microscopy (HRTEM). The metabasites contain a small quantity of fine-grained smectite and corrensite in the <1 μm size fraction. The chlorite also contains trace amounts of Ca, Na and K, which generally appear to be associated with smectite stacked in chlorite packets. The smectite layers comprise up to 13% of the chlorite domains. Theoretical estimates of the smectite ratio by the Wise method using EMPA data coincide well with the ratio determined based on HRTEM observations in most chlorites. However, in some chlorites with high proportions of Ca, Na and K, the cations cannot be reasonably attributed to smectite alone. Based on the present analyses, Ca, Na and K cations are also hosted in discrete interstitial phases of fine-grained smectite and corrensite as possible retrograde metamorphic products. These findings suggest that care should be taken in application of the Wise method to estimate the smectite ratio, and that the whole-rock chlorite composition may not be suitable as a geothermometer.

Key Words—Chlorite, Corrensite, EMPA, HRTEM, Japan, Metabasite, Smectite, XRD.

INTRODUCTION

Chlorite is formed ubiquitously in the processes of diagenesis, low-grade metamorphism and hydrothermal alteration (*e.g.* Foster, 1962; McDowell and Elders, 1980; Inoue and Utada, 1991; Buatier *et al.*, 1995; Schmidt *et al.*, 1999). The chemical composition of chlorite is complex, varying with temperature, whole-rock chemical composition, and mode of occurrence (*e.g.* Hillier and Velde, 1991; Bevins *et al.*, 1991). The tetrahedral Al occupancy in chlorite has therefore been proposed as an empirical chlorite geothermometer (*e.g.* Cathelineau and Nieva, 1985; Cathelineau, 1988; Xie *et al.*, 1997; López-Munguira *et al.*, 2002). However, this geothermometer is affected by the presence of Ca, Na and K cations, which are not essential elements in chlorite but are often present in trace amounts (Jiang *et al.*, 1994; Martinez-Serrano and Dubois, 1998; Schmidt *et al.*, 1999). Ca, Na and K cations are much larger than Si, Al, Fe and Mg, and it therefore seems impossible for these cations to occupy the tetrahedral and octahedral sites of chlorite. These cations are generally believed to originate from smectite layers in the chlorite, and the ratio of smectite in the chlorite can be estimated by the Wise method based on data for Ca, Na and K obtained through chemical analysis (Bettison and Schiffman, 1988; Bevins *et al.*, 1991; Bettison *et al.*, 1991). However, the accuracy of such estimation remains to be determined. According to Jiang *et al.* (1994), Ca, Na and K in chlorite originate from not only smectite layers in the chlorite itself but also other rock-forming minerals such as calcite and albite, which form discrete phases in the chlorite aggregate. Determination of the origin of Ca, Na and K in chlorite is therefore a complex issue.

In the Mikabu and North Chichibu belts of southwest Japan, metamorphosed basic rocks (metabasites) containing significant abundances of chlorite and actinolite are prevalent. Chlorite occurs mainly as the replacement of phenocrysts in the metabasites. In this study, several metabasite samples were collected from the Mikabu and North Chichibu belts, and the chemical compositions of chlorites in these metabasite samples were obtained by EMPA. The stacking structures of the chlorites were also clarified by HRTEM. The primary purpose of this study is to compare the theoretically estimated smectite component ratio with the observed ratio in order to clarify the origin of Ca, Na and K in the chlorite.

GEOLOGICAL SETTING

The Mikabu belt

The Mikabu belt is distributed from the Kanto mountain range to western Shikoku Island along the southern rim of the Sanbagawa belt (Figure 1). The Mikabu belt comprises the Mikabu green rocks which have been identified, through petrological and geochemical studies, as being ophiolitic, possibly representing an ophiolite complex thrust up onto a seamount or sea

* E-mail address of corresponding author:
miyahara@ganko.tohoku.ac.jp
DOI: 10.1346/CCMN.2005.0530504

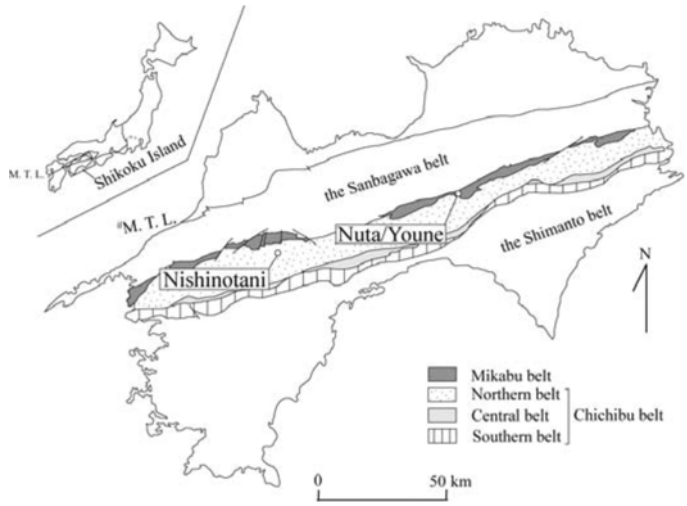

Figure 1. Schematic geotectonic map of Shikoku Island (after Takeda, 1984). # M. T. L. = Median Tectonic Line.

plateau (Morikiyo, 1979; Takeda, 1984; Isozaki *et al*., 1990; Ozawa *et al*., 1999).

On Shikoku Island, the lenticular rock masses of the Mikabu green rocks are distributed between the Sanbagawa belt and the Chichibu belt (Figure 1). It has been estimated that the original Mikabu green rock sediments distributed on Shikoku Island are pre-Triassic in age (*e.g*. Suyari *et al*., 1980, 1982). According to K/Ar and Ar/Ar isotope geochronological data obtained for metamorphic white mica in phyllite and for whole-rock phyllite, the Mikabu green rocks appear to have undergone metamorphism in the period from the early to middle Cretaceous (Kawato *et al*., 1991; Dallmeyer *et al*., 1995).

The North Chichibu belt

As shown in Figure 1, the Chichibu belt is divided into northern, central and southern regions based on properties such as the tectonic zone, rock facies and geological age of the rocks (*e.g*. Matsuoka, 1985; Isozaki and Itaya, 1990). The North Chichibu belt is composed of sandstone, slate, chert, limestone and green rock (*e.g*.

Table 1. Phyllosilicate assemblages of metabasites as determined by XRD analyses (−: not detected, x: small quantity, xx: medium quantity, xxx: abundant).

Locality	Borehole	Depth (m)	Origin	Bulk-rock #Fe/(Fe+Mg)	Clay fraction composition (<1 μm) Smectite	Corrensite	Chlorite
Nuta/Youne	Y2-31	30.4	basalt		x	–	xxx
		31.45	basalt	0.16	xx	–	xxx
		39.0	basalt		x	–	xxx
		48.4	hyaloclastite	0.14	xx	–	xxx
		52.4	dolerite	0.14	x	–	xxx
		59.7	basalt	0.21	x	xx	xxx
		62.25	basalt		–	–	xxx
		70.6	basalt	0.15	x	–	xxx
		77.4	basalt		–	–	xxx
		82.2	basalt		xx	x	xxx
		102.0	basalt	0.12	–	–	xxx
Nishinotani	II–2	16.5	basalt	0.16	x	–	xxx
	IIe–3	20.8	basalt	0.17	xx	x	xxx
		27.6	basalt	0.18	xx	xx	xxx
	IIi–1	53.7	basalt	0.15	x	–	xxx
	IIj–1	47.2	basalt	0.16	xx	–	xxx
	IIj–2	23.1	basalt	0.17	x	–	xxx
		28.6	basalt	0.17	x	–	xxx

Bulk-rock Fe/(Fe+Mg) ratio is from Miyahara (2004).

https://doi.org/10.1346/CCMN.2005.0530504 Published online by Cambridge University Press

Kashima, 1969; Murata, 1982), the last of which appears to be the Mikabu green rocks (Suzuki and Ishizuka, 1998). It is considered that the North Chichibu belt underwent low-grade Sanbagawa metamorphism akin to that in the Mikabu belt (*e.g.* Suzuki, 1972; Maruyama and Liou, 1985; Banno and Sakai, 1989).

MATERIALS

Many drillings have been conducted in the Mikabu and North Chichibu belts as part of landslide control work. In this study, some of the least-disturbed cores obtained from these drillings were selected for specimen collection, and specimens exhibiting the least weathering were taken for analysis. A total of 11 metabasite samples (Mikabu green rocks) were collected from borehole Y2-31 in the Nuta/Youne Landslide area of the Mikabu belt, and seven metabasite samples were collected from boreholes II-2, IIe-3, IIi-1, IIj-1 and IIj-2 in the Nishinotani Landslide area of the North Chichibu belt (Figure 1).

Most of the metabasite samples are deemed to have originated from basalt (Table 1) with a typical blastoporphyritic texture (Figure 2a), and most of the phenocrysts in the metabasites exhibit lenticular or laminar deformation. The phenocrysts are predominantly replaced by chlorite (Figure 2b), although some actinolite, clinopyroxene (augite and diopside), hematite, pyrite and chalcopyrite replacement is also recognized in the phenocrysts. The groundmass consists of clinopyroxene (augite and diopside), actinolite and minor chlorite, plagioclase, Na pyroxene, alkali amphibole, olivine, quartz, calcite, hematite, pyrite, chalcopyrite and titanite.

EXPERIMENTAL METHODS

X-ray powder diffraction (XRD) analyses were performed on the clay fraction (<1 μm) extracted from whole rock by ultrasonic dispersion of specimens in deionized water followed by centrifugation. The samples were oriented by placing the clay suspension on Na glass and drying at room temperature. Clay minerals were subjected to a variety of treatments as recommended by Moore and Reynolds (1997): (1) Mg saturation, (2) glycerol solvation, and (3) heating at 300 and 500ºC. Two representative specimens were selected, and each was divided into six size fractions (<0.2, 0.2–0.5, 0.5–1.0, 1.0–2.0, 2.0–5.0 and 5.0–20 μm) using a high-speed centrifuge. Conventional XRD measurements were conducted on a MAC Science M18XHF diffractometer equipped with a graphite monochromator (CuKα radiation; 40 kV; 100 mA). The oriented samples were scanned over the interval 2–50º2θ at a scanning speed of 2º/min in 0.02º2θ steps. The divergence, scattering and receiving slits were 0.5º, 0.5º and 0.15 mm, respectively.

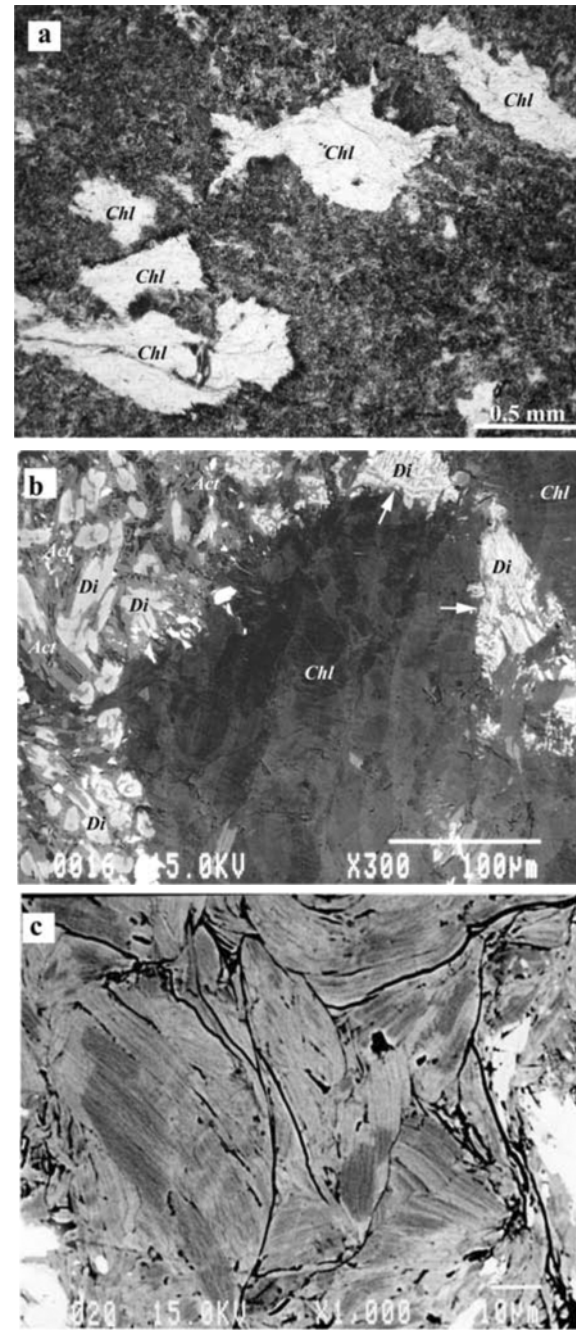

Figure 2. Representative specimen from Y2-31 82.2m. (a) Photomicrograph showing a blastoporphyritic texture. The phenocrysts are mainly replaced by chlorites. (b) BSE image exhibits chlorite as the replacement of phenocryst. Clinopyroxene is replaced by actinolite. A dendritic clinopyroxene is indicated by white arrows. (c) Chlorite is featured by a chemical compositional zonation. Chl: chlorite; Act: actinolite; Di: diopside.

Wavelength-dispersive EMPA of phyllosilicates in polished thin-sections was carried out using a JEOL JCMA-733II electron microprobe. Analyses were carried out using an accelerating voltage of 15 kV, a beam current of 12 nA and a spot size of 5 μm to reduce beam

https://doi.org/10.1346/CCMN.2005.0530504 Published online by Cambridge University Press

damage and loss of alkali ions. Wollastonite (Si and Ca), rutile (Ti), corundum (Al), hematite (Fe), manganosite (Mn), eskolaite (Cr), periclase (Mg), albite (Na) and adularia (K) were used as standards.

Samples for HRTEM were selected from double-polished petrographic thin-sections ~30 μm thick. Following the method of Miyahara and Ishisako (2004), a 3 mm Mo grid was attached to the area to be observed in the thin-section, and after removal of the grid the section was thinned to electron transparency by argon ion milling. A JEOL-2010 transmission electron microscope (200 kV) was used for observing lattice fringe images in an overfocus condition.

RESULTS

X-ray powder diffraction analyses

Size fraction. The XRD analyses reveal three assemblages of phyllosilicates in the metabasites: (1) chlorite, (2) smectite + chlorite, and (3) smectite + corrensite + chlorite (Table 1). The data for two representative specimens in the six size fractions are shown in Figure 3. These specimens were Mg-saturated and glycerol-solvated. Chlorite is dominant in all size fractions, whereas smectite and corrensite are concentrated in the fined-grained (<1 μm) fraction.

Chlorite, smectite and corrensite. The d_{001} value of the chlorite did not change upon Mg or K saturation or glycerol solvation (Figure 4). Strong 0.154 nm and weak 0.151 nm reflections suggest that the former is the 060 reflection of chlorite (not shown), and the intensity of the 060 reflection suggests a trioctahedral phase.

Mg-saturated smectite has a d_{001} value of ~1.4 nm, which expands to ~1.8 nm upon glycerol solvation (Figure 4). It is assumed that a small amount of vermiculite-like smectite is present, as d_{001} for K-saturated smectite is indicated by successive reflections with a shoulder at 1.0 nm. Strong 0.154 nm and weak 0.151 nm reflections were also recognized as the 060 reflection for smectite, indicating that most smectite was trioctahedral.

The d_{001} value of Mg-saturated corrensite is ~2.9 nm, shifting to ~3.2 nm upon glycerol solvation (Figure 4). The intensity of the d_{001} reflection was remarkably lower for K-saturated corrensite. It is inferred that K-saturated smectite contained in corrensite varies from 1.0 to 1.3 nm because the layer charge of the smectite component included in corrensite is heterogeneous. Accordingly, the symmetry along the *c* axis of K-saturated corrensite is low, resulting in the weaker d_{001} reflection.

EMPA analyses

Chlorite generally occurs as a replacement of phenocrysts in metabasites. Chlorite formed from such phenocrysts are typically colorless, light green or brown under the polarizing microscope, and exhibit anomalous interference colors such as ash gray under crossed polars. Some aggregated chlorites also display other optical features.

Back-scattered electron (BSE) images of chlorite in the present examples reveal unambiguous chemical compositional zonation (Figure 2c), where light areas correspond to a slight enrichment of Fe. The compositional zonation is remarkable in chlorite from metabasite samples from borehole Y2-31 (Figure 2c).

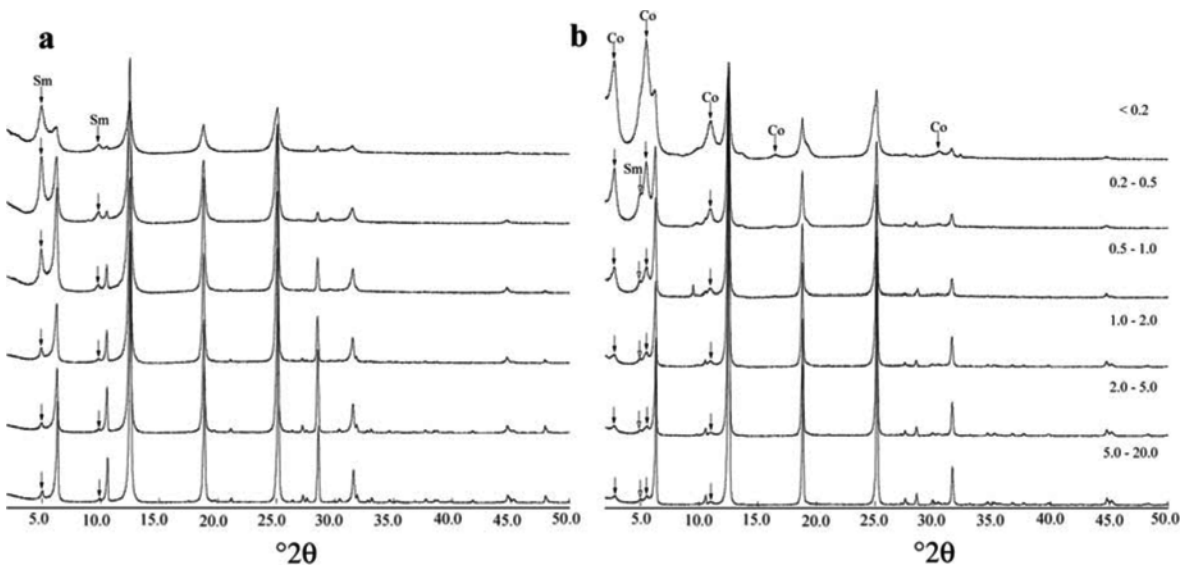

Figure 3. XRD patterns (CuKα) of $MgCl_2$ + glycerol-solvated <0.2, 0.2–0.5, 0.5–1.0, 1.0–2.0, 2.0–5.0 and 5.0–20.0 μm size fractions for: (a) chlorite + smectite (Sm). Specimen from Y2-31, 31.45m; and (b) chlorite + corrensite (Co) + smectite (Sm). Specimen from Y2-31, 59.7 m. Although smectite is also contained in the <0.2 μm size fraction, its d_{001} reflection is ambiguous because it is overlapped by the reflection of corrensite.

https://doi.org/10.1346/CCMN.2005.0530504 Published online by Cambridge University Press

The results of EMPA chemical analyses of chlorites formed in phenocrysts were recalculated based on 28 oxygens (Table 2), assuming that all Fe was ferrous. Ferric Fe is a minor constituent in low-grade metamorphic chlorite and its presence in small amounts is of little consequence for the purpose of comparing compositions (Black, 1975; Cathelineau and Nieva, 1985; Martinez-Serrano and Dubois, 1998).

Tetrahedral Si cation content ranges from 5.62 to 6.68 per chlorite unit (Table 2), and the $Fe^{2+}/(Fe^{2+}+Mg)$ ratio ranges from 0.19 to 0.37. Although the chlorite is generally clinochlore (Bailey, 1980), it is classified into brunsvigite, clinochlore, diabantite and penninite based on a Foster-type diagram (Foster, 1962). The maximum number of Ca cations per chlorite unit is 0.49 (Table 2), and Na and K cations are present in trace amounts. The total (Ca+Na+K) content reaches 0.63 per chlorite unit.

HRTEM observations and interpretations

1.4 nm layers. The lattice fringes of chlorite are very well defined, and the contrast is high. Chlorite formed in the phenocrysts consists of aggregated chlorite packets, which occur as domains 200–300 nm wide.

1.0 nm layer stacked in chlorites. A few lattice fringes with a periodicity of 1.0 nm are observed within the chlorite packets (Figure 5). Up to three repetitions of the chlorite-like layer and 1.0 nm layer pair occur in these samples, and successive 1.0 nm layers are not observed. The chlorite domains observed by HRTEM consist of no more than 13% of these 1.0 nm layers (Figure 6).

Klimentidis and Mackinnon (1986) reported that smectite layers collapse to 1.0–1.2 nm due to dehydration in the vacuum produced by HRTEM. This feature

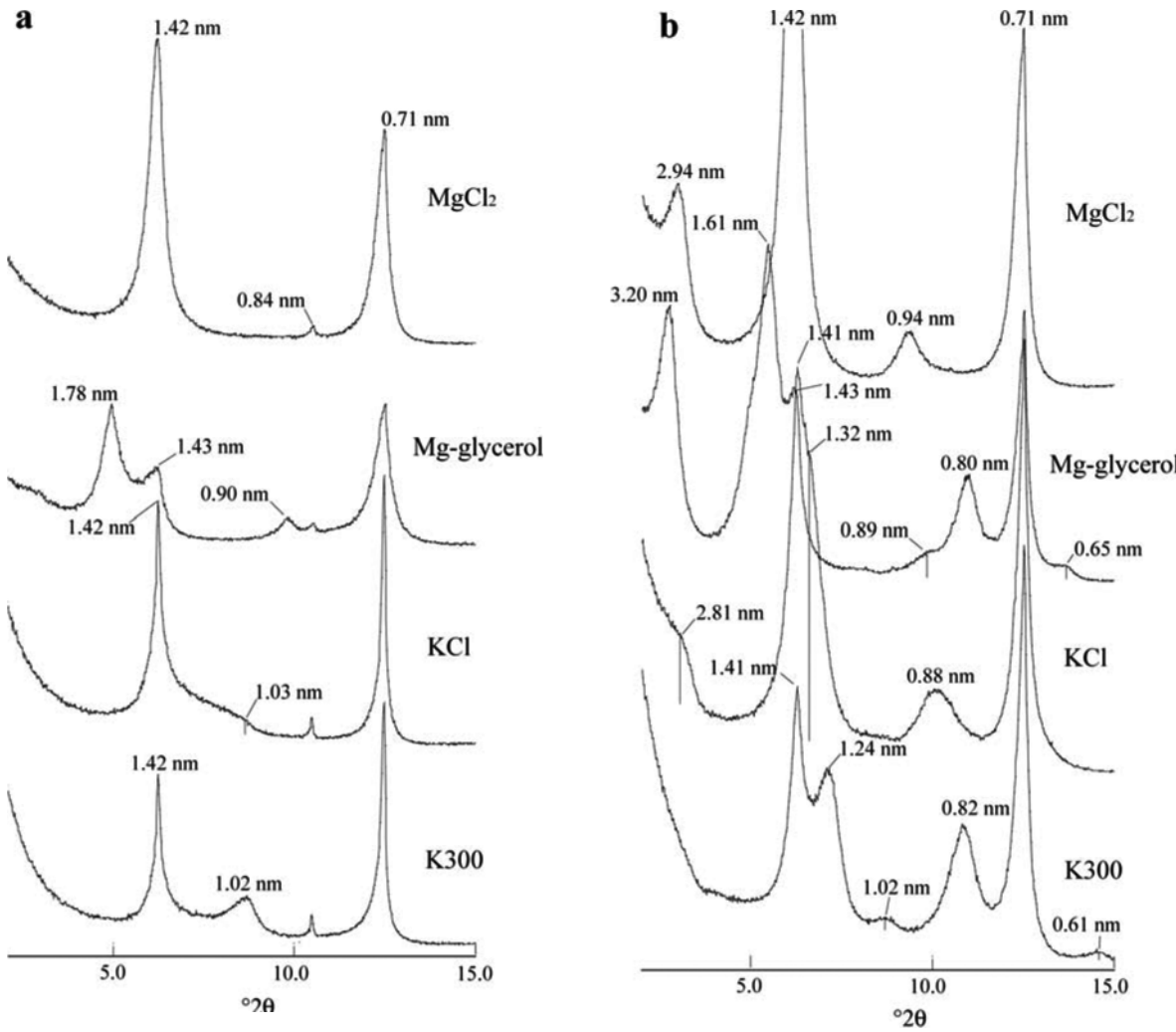

Figure 4. Representative XRD patterns (CuKα) of <0.2 μm size fractions ($MgCl_2$-solvated, $MgCl_2$ + glycerol-solvated (= 'Mg-glycerol'), KCl-solvated and KCl + heated to 300°C (= 'K300') for: (a) chlorite + smectite. Specimen from Y2-31, 31.45 m, and (b) chlorite + corrensite + #(smectite). Specimen from Y2-31, 59.7 m. $d = 0.84$ nm reflection is actinolite of the clay size-fraction. # See caption in Figure 3.

https://doi.org/10.1346/CCMN.2005.0530504 Published online by Cambridge University Press

allows smectite to be distinguished from chlorite in the present analysis. However, it has also been reported that another phyllosilicate having a periodicity of ~1.0 nm, such as illite or talc, may also be stacked in chlorite (Ahn and Peacor, 1985; Sharp and Buseck, 1988; Shau and Peacor, 1992). Therefore, the 1.0 nm layer needs to be interpreted carefully by comparison with EMPA analyses (Table 2).

In most chlorite formed in phenocrysts, the (Ca+Na+K) content is <0.10 per 28O unit. Generally, such small abundances of Ca, Na and K cations are ignored (*e.g.* Martínez-Serrano and Dubois, 1998; Zane *et al.*, 1998; Barrenechea *et al.*, 2000). The K cation is scarce in the present chlorite examples (except for a result of 0.09 in one analysis), indicating that micas such as illite and biotite are unlikely to be stacked in the chlorite domains. Assuming that a talc layer is present in the chlorite domains, the Si content would increase without a parallel increase in (Ca+Na+K). As shown in Figure 7, however, this feature is ambiguous in the present chlorites. Although fine-grained smectite and corrensite were detected by XRD analysis, the intergrowth of smectite or corrensite with chlorite was not observed by HRTEM. Nevertheless, as shown in Figure 7, tetrahedral Si seems to be correlated with the (Ca+Na+K) content. Considering the lower Al/Si ratio of

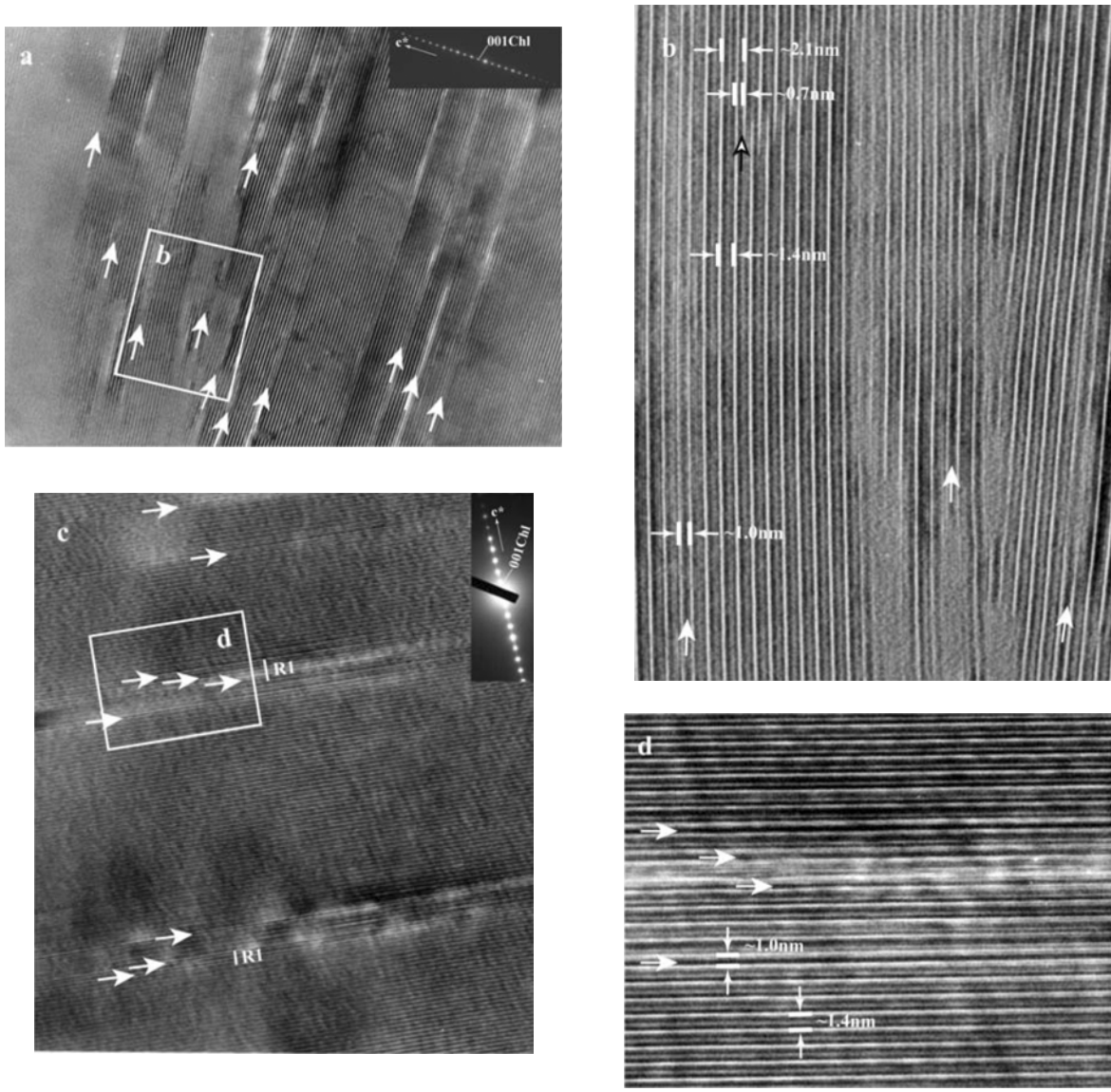

Figure 5. HRTEM images of chlorite formed in a phenocryst. 1.0 nm layers are indicated by white arrows. (a) R0 Chl-1.0 nm layer. Specimen from Y2-31, 52.4 m. (b) 0.7 nm layer indicated by a fringed arrow. (c) Small R1 Chl-1.0 nm layer domains in a chlorite packet. Specimen from Y2-31, 39 m. (d) A magnified portion of part c.

https://doi.org/10.1346/CCMN.2005.0530504 Published online by Cambridge University Press

Table 2. Representative EMPA analyses of phyllosilicates (borehole Y2-31: the Mikabu belt; boreholes II-2, IIe-3, IIi-1, IIj-1, IIj-2: the north Chichibu belt).

Borehole	Y2-31																
	5-68	5-42	4-31	3-103	6-126	6-127	3-63	3-50	1-21	1-25	5-13	6-104	6-110	6-116	6-120	6-112	6-115
Depth (m)	30.4	30.4	31.45	31.45	39	39	48.4	48.4	52.4	52.4	59.7	62.25	62.25	70.6	70.6	77.4	77.4
SiO_2	32.35	33.12	30.38	31.47	29.60	29.34	29.76	30.92	30.97	31.67	27.80	29.41	29.69	29.12	28.42	29.65	29.33
TiO_2	0.05	0.05	0.12	0.06	0.00	0.00	0.00	0.00	0.07	0.00	0.00	0.01	0.03	0.00	0.03	0.06	0.04
Al_2O_3	15.12	15.18	16.39	16.09	17.97	18.17	17.17	16.72	14.97	13.27	19.21	16.97	17.92	17.95	16.50	17.00	18.39
FeO*	16.80	16.82	14.90	15.64	16.11	15.64	15.63	15.19	13.50	11.79	21.57	16.35	16.09	16.70	16.73	16.01	16.29
MnO	0.19	0.15	0.28	0.18	0.22	0.23	0.17	0.20	0.07	0.12	0.32	0.26	0.23	0.22	0.25	0.25	0.25
Cr_2O_3	1.07	0.00	0.36	0.96	0.33	0.31	0.23	0.12	0.42	1.23	0.03	1.49	0.70	0.28	4.12	0.79	0.11
MgO	22.05	23.05	24.62	24.29	24.67	24.16	25.13	25.13	27.45	28.98	20.39	24.47	24.69	23.61	22.70	24.32	24.56
CaO	1.73	0.30	0.16	0.66	0.03	0.16	0.03	0.14	0.11	0.07	0.07	0.04	0.08	0.15	0.06	0.08	0.08
Na_2O	0.13	0.25	0.04	0.09	0.01	0.03	0.00	0.01	0.00	0.01	0.02	0.03	0.00	0.00	0.02	0.01	0.00
K_2O	0.06	0.34	0.07	0.02	0.06	0.03	0.03	0.08	0.00	0.04	0.00	0.04	0.06	0.05	0.00	0.01	0.01
Total (wt.%)	89.55	89.25	87.30	89.46	89.00	88.07	88.14	88.50	87.56	87.17	89.41	89.07	89.49	88.07	88.83	88.17	89.06
Si	6.38	6.51	6.08	6.17	5.84	5.84	5.91	6.09	6.13	6.27	5.62	5.84	5.83	5.83	5.72	5.92	5.79
^{IV}Al	1.62	1.49	1.92	1.83	2.16	2.16	2.09	1.91	1.87	1.73	2.38	2.16	2.17	2.17	2.28	2.08	2.21
Σtet	8.00	8.00	8.00	8.00	8.00	8.00	8.00	8.00	8.00	8.00	8.00	8.00	8.00	8.00	8.00	8.00	8.00
^{VI}Al	1.90	2.02	1.94	1.88	2.02	2.10	1.94	1.98	1.63	1.36	2.20	1.81	1.98	2.07	1.64	1.91	2.06
Ti	0.01	0.01	0.02	0.01	0.00	0.00	0.00	0.00	0.01	0.00	0.00	0.00	0.00	0.00	0.00	0.01	0.01
Fe	2.77	2.76	2.49	2.56	2.66	2.60	2.60	2.50	2.24	1.95	3.65	2.71	2.64	2.80	2.82	2.67	2.69
Mn	0.03	0.02	0.05	0.03	0.04	0.04	0.03	0.03	0.01	0.02	0.06	0.04	0.04	0.04	0.04	0.04	0.04
Cr	0.17	0.00	0.06	0.15	0.05	0.05	0.04	0.02	0.07	0.19	0.00	0.23	0.11	0.04	0.66	0.12	0.02
Mg	6.49	6.75	7.34	7.10	7.26	7.17	7.45	7.38	8.10	8.55	6.15	7.24	7.23	7.05	6.81	7.23	7.23
Σoct	11.37	11.57	11.90	11.73	12.03	11.96	12.05	11.91	12.05	12.07	12.06	12.04	12.01	11.99	11.97	11.99	12.04
oct-vacancy	0.63	0.43	0.10	0.27	–0.03	0.04	–0.05	0.09	–0.05	–0.07	–0.06	–0.04	–0.01	0.01	0.03	0.01	–0.04
Fe^{2+}/(Fe^{2+}+Mg)	0.30	0.29	0.25	0.27	0.27	0.27	0.26	0.25	0.22	0.19	0.37	0.27	0.27	0.28	0.29	0.27	0.27
Ca	0.37	0.06	0.03	0.14	0.01	0.03	0.01	0.03	0.02	0.01	0.02	0.01	0.02	0.03	0.01	0.02	0.02
Na	0.05	0.10	0.01	0.03	0.00	0.01	0.00	0.00	0.00	0.00	0.01	0.01	0.00	0.00	0.01	0.00	0.00
K	0.01	0.09	0.02	0.00	0.02	0.01	0.01	0.02	0.00	0.01	0.00	0.01	0.02	0.01	0.00	0.00	0.00
Ca+Na+K	0.43	0.24	0.07	0.18	0.02	0.05	0.01	0.05	0.02	0.03	0.02	0.03	0.03	0.04	0.02	0.02	0.02
Chlorite ratio (x)**	0.66	0.77	0.95	0.86	1.02	0.98	1.03	0.95	1.04	1.05	1.04	1.03	1.01	1.00	1.01	1.00	1.03
Smectite ratio ($1-x$)	0.34	0.23	0.05	0.14	–0.02	0.02	–0.03	0.05	–0.04	–0.05	–0.04	–0.03	–0.01	0.00	–0.01	0.00	–0.03

All recalculation based on 28 oxygens. * FeO as total iron. ** Chlorite ratio (x) from the Wise method

smectite compared to chlorite (*e.g.* Bettison and Schiffman, 1988; Schiffman and Fridleifsson, 1991), the unambiguous relationship between octahedral vacancies and the (Ca+Na+K) content (Figure 8), and the lower oxygen content in smectite (22) compared to chlorite (28), the 1.0 nm layers in the chlorite are concluded to represent collapsed smectite layers.

0.7 nm layers. A few lattice fringes with spacing of ~0.7 nm were identified within the chlorite packets (Figure 5b). The 0.7 nm layers never appeared in succession, and did not generally contact the 1.0 nm layer. This 0.7 nm layer is also less abundant than the 1.0 nm layer (Figure 6).

This layer may represent either kaolin or serpentine, which are difficult to distinguish by HRTEM due to the strong similarity of the lattice fringe images of these two minerals under all defocusing conditions (Guthrie and Veblen, 1990). According to Jiang and Peacor (1991), kaolinite becomes amorphous under HRTEM within a few seconds due to interaction with the electron beam. However, the 0.7 nm layer observed in the present samples survived for at least a few minutes. Furthermore, in a mafic environment, it seems improbable that a kaolin-like layer, rich in Si and Al, would have formed in the chlorite packets. The 0.7 nm layer is therefore presumed to represent serpentine.

Berthierine, a 0.7 nm Fe,Mg alumino-silicate, is also found in metapelites and metabasites as a potential precursor of Fe chlorite (Mata *et al*., 2001; Jiang *et al*., 1992). This assignment has been confirmed in published synthesis experiments (James *et al*., 1976; Fawcett and Yoder, 1966). Mata *et al*. (2001) proposed that the occurrence of berthierine in chlorite packets depends on the Fe-rich bulk-rock chemical composition. As the present metabasites are rich in Mg (Table 1), the 0.7 nm layer is more likely to be lizardite than berthierine.

DISCUSSION

Origin of Ca, Na and K cations in chlorite

The proportions of chlorite and smectite in the chlorite-smectite mixed-layer mineral can be estimated by the Wise method using EMPA data (Bettison and

https://doi.org/10.1346/CCMN.2005.0530504 Published online by Cambridge University Press

Table 2. *Continued.*

Borehole	Y2-31				II-2		IIe-3			IIi-1		IIj-1		IIj-2	
	5-77	5-78	2-50	2-65	7-57	7-56	7-22	7-16	7-47	7-73	7-84	7-54	7-63	7-33	7-24
Depth (m)	82.2	82.2	102	102	16.5	16.5	20.8	20.8	27.6	53.7	53.7	47.2	47.2	23.1	28.6
SiO_2	30.98	34.59	29.85	29.11	32.80	32.80	33.19	33.48	31.20	30.31	31.96	30.20	30.52	29.36	33.09
TiO_2	0.01	0.03	0.00	0.00	0.00	0.00	0.00	0.00	0.00	0.03	0.04	0.00	0.00	0.00	0.00
Al_2O_3	14.96	13.71	18.82	18.65	15.92	15.98	15.07	15.38	15.55	17.13	16.49	16.33	16.53	16.44	13.97
FeO*	11.83	14.09	12.54	12.87	15.35	15.71	15.49	15.97	16.74	13.29	15.24	16.40	16.17	16.45	17.20
MnO	0.21	0.18	0.13	0.19	0.19	0.20	0.21	0.18	0.28	0.21	0.19	0.32	0.27	0.26	0.22
Cr_2O_3	0.24	0.08	0.14	0.80	0.40	0.29	0.00	0.00	0.00	0.31	0.23	0.08	0.46	1.19	0.00
MgO	26.73	24.56	26.94	26.59	23.14	23.89	23.76	24.42	23.55	24.72	24.28	24.67	24.80	24.13	23.52
CaO	0.14	2.39	0.03	0.03	1.25	1.06	0.24	0.32	0.35	0.14	0.83	0.82	0.11	0.12	0.30
Na_2O	0.01	0.27	0.00	0.01	0.17	0.09	0.31	0.19	0.00	0.02	0.03	0.00	0.00	0.00	0.00
K_2O	0.03	0.13	0.01	0.01	0.00	0.00	0.26	0.22	0.00	0.03	0.02	0.00	0.00	0.00	0.02
Total (wt.%)	85.12	90.03	88.45	88.27	89.21	90.01	88.52	90.16	87.66	86.18	89.31	88.82	88.86	87.95	88.32
Si	6.25	6.68	5.81	5.71	6.41	6.36	6.53	6.48	6.26	6.08	6.24	6.00	6.03	5.90	6.58
^{IV}Al	1.75	1.32	2.19	2.29	1.59	1.64	1.47	1.52	1.74	1.92	1.76	2.00	1.97	2.10	1.42
Σtet	8.00	8.00	8.00	8.00	8.00	8.00	8.00	8.00	8.00	8.00	8.00	8.00	8.00	8.00	8.00
^{VI}Al	1.81	1.80	2.12	2.02	2.08	2.02	2.03	1.98	1.93	2.13	2.03	1.82	1.88	1.80	1.85
Ti	0.00	0.00	0.00	0.00	0.00	0.00	0.00	0.00	0.00	0.00	0.01	0.00	0.00	0.00	0.00
Fe	1.99	2.27	2.04	2.11	2.51	2.55	2.55	2.58	2.81	2.23	2.49	2.72	2.67	2.77	2.86
Mn	0.04	0.03	0.02	0.03	0.03	0.03	0.03	0.03	0.05	0.03	0.03	0.05	0.05	0.04	0.04
Cr	0.04	0.01	0.02	0.12	0.06	0.04	0.00	0.00	0.00	0.05	0.04	0.01	0.07	0.19	0.00
Mg	8.04	7.07	7.81	7.78	6.74	6.91	6.97	7.04	7.04	7.39	7.07	7.30	7.31	7.23	6.97
Σoct	11.92	11.19	12.02	12.06	11.43	11.55	11.58	11.64	11.83	11.83	11.66	11.91	11.98	12.03	11.72
oct-vacancy	0.08	0.81	–0.02	–0.06	0.57	0.45	0.42	0.36	0.17	0.17	0.34	0.09	0.02	–0.03	0.28
$Fe^{2+}/(Fe^{2+}+Mg)$	0.20	0.24	0.21	0.21	0.27	0.27	0.27	0.27	0.29	0.23	0.26	0.27	0.27	0.28	0.29
Ca	0.03	0.49	0.01	0.01	0.26	0.22	0.05	0.07	0.07	0.03	0.17	0.17	0.02	0.02	0.06
Na	0.00	0.10	0.00	0.00	0.06	0.03	0.12	0.07	0.00	0.01	0.01	0.00	0.00	0.00	0.00
K	0.01	0.03	0.00	0.00	0.00	0.00	0.07	0.06	0.00	0.01	0.00	0.00	0.00	0.00	0.00
Ca+Na+K	0.04	0.63	0.01	0.01	0.33	0.25	0.23	0.19	0.07	0.04	0.19	0.17	0.02	0.02	0.07
Chlorite ratio (x)**	0.95	0.57	1.01	1.04	0.69	0.75	0.77	0.80	0.90	0.91	0.81	0.95	0.99	1.03	0.84
Smectite ratio ($1-x$)	0.05	0.43	–0.01	–0.04	0.31	0.25	0.23	0.20	0.10	0.09	0.19	0.05	0.01	–0.03	0.16

Schiffman, 1988; Bevins *et al.*, 1991; Bettison *et al.*, 1991). Bettison and Schiffman (1988) compared the chlorite component ratios estimated theoretically by the Wise method and from XRD patterns. However, the smectite component ratio estimated by the Wise method has yet to be correlated quantitatively with the smectite-like layers observed by HRTEM.

The compositional ratios of chlorite and smectite were estimated by the Wise method assuming that the present chlorite is a tri-chlorite-tri-smectite mixed-layer mineral. The smectite ratio determined in this way reaches a maximum of 43% (Table 2). In most chlorites, the (Ca+Na+K) content is no greater than 0.10 per chlorite unit. At (Ca+Na+K) abundances below 0.1, the smectite ratio only reaches 10% (Figure 9). It should be noted that the estimated smectite ratio is very similar to the maximum ratio of smectite layers determined by HRTEM observation (Figure 6). It is therefore concluded that in specimens with a (Ca+Na+K) content of <0.10 per chlorite unit, Ca, Na and K are present in the smectite layers.

The proportion of smectite in chlorite from metabasic rocks from the Bükk Mountains, northeastern Hungary, has been estimated to be 4–12% in the anchizone and 1–8% in the epizone (Árkai and Ghabrial, 1997). Combined TEM and analytical electron microscopy (AEM) have revealed that saponite layers in chlorite from the volcanogenic Taveyanne metasediment of the western Helvetic nappes, Switzerland, are present at up to ~7% in the anchizone and ~2% or less in the epizone (Schmidt *et al.*, 1999). In consideration of these results, chlorite containing <10% smectite in the pumpellyite-actinolite or lower-greenschist facies appears to be of non-local origin.

In some of the present chlorite samples, the (Ca+Na+K) content exceeds 0.10 per chlorite unit. In these samples, the estimated smectite ratio increases from 10 to 43% with an increase in (Ca+Na+K) content from 0.10 to 0.63. However, chlorite containing such large proportions of smectite was not recognized by either XRD or HRTEM observations. Despite the unambiguous relationship between the octahedral vacancies and the (Ca+Na+K) content in chlorites, it is unlikely that such large abundances of Ca, Na and K can be hosted by the smectite layers alone.

It is possible that the abnormal (Ca+Na+K) content in the chlorite is present in fine-grained smectite and corrensite (Figure 10). In the interstices (100–200 nm

https://doi.org/10.1346/CCMN.2005.0530504 Published online by Cambridge University Press

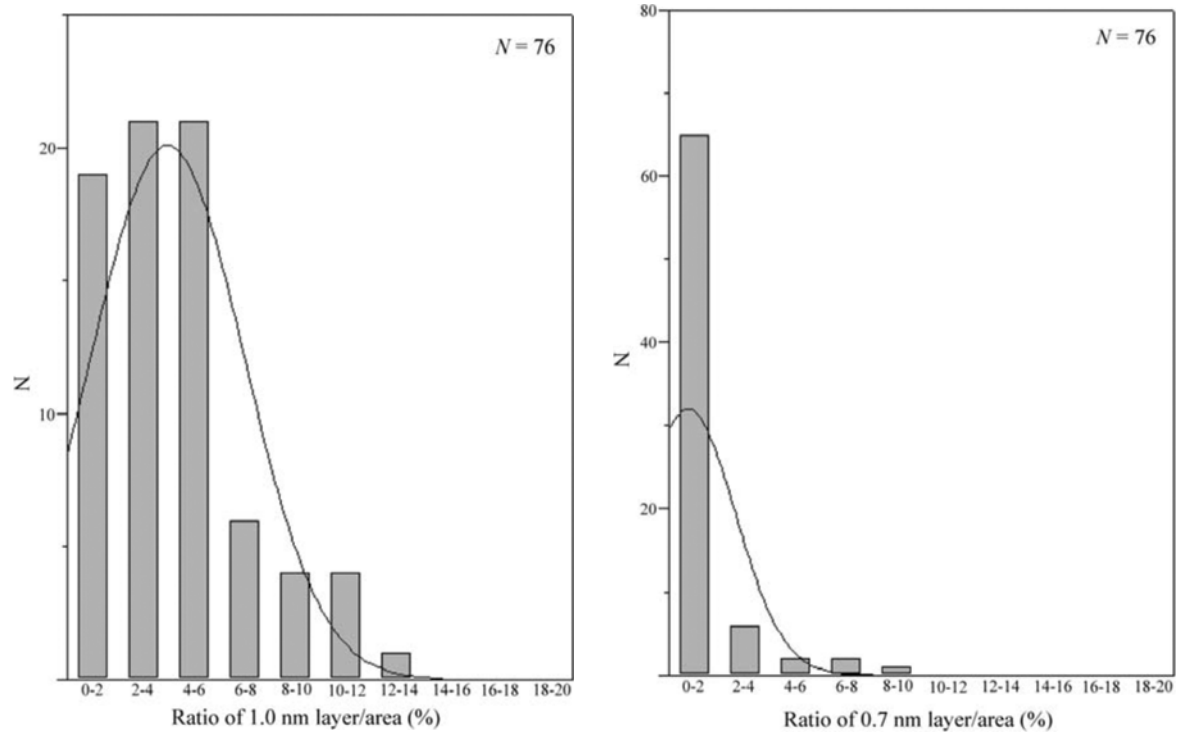

Figure 6. The frequency distribution of 1.0 nm and 0.7 nm layers in chlorite phenocrysts. 1.0 nm and 0.7 nm layers are at a maximum of 13% and 8%, respectively. The ratios of 1.0 nm and 0.7 nm layers were taken from the Y2-31 samples at 31.45 m, 39 m, 52.4 m, 59.7 m, 77.4 m, 82.2 m and 102 m and the IIi-1 sample at 53.7 m.

wide) of Ca- and Na-rich chlorite, several corrensite packets are recognized in these examples (Figure 11). Such microscopic interstices are difficult to identify by EMPA. Smectite may also have formed in microscopic interstices.

According to Banno and Sakai (1989), the peak metamorphic conditions of the present study are 250–300ºC and 5–6 kbar. Previous reports suggest that the fine-grained smectite and corrensite in this region occur as metastable or unstable phases under such *P-T* conditions (Inoue and Utada, 1991; Schiffman and Fridleifsson, 1991; reviewed in Alt, 1999). The fine-grained smectite and corrensite is therefore considered to represent a retrograde metamorphic product, *i.e.* Ca, Na and K occur in smectite layers in some chlorite packets, and as fine-grained smectite and corrensite formed during retrograde metamorphism in other aggregates.

Chlorite geothermometer

The tetrahedral Al occupancy in chlorite is dependent on the formation temperature (McDowell and Elders,

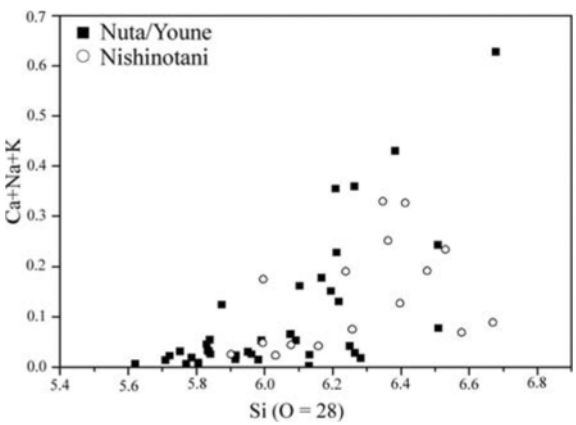

Figure 7. Si *vs.* (Ca+Na+K) content plots for chlorite in phenocrysts.

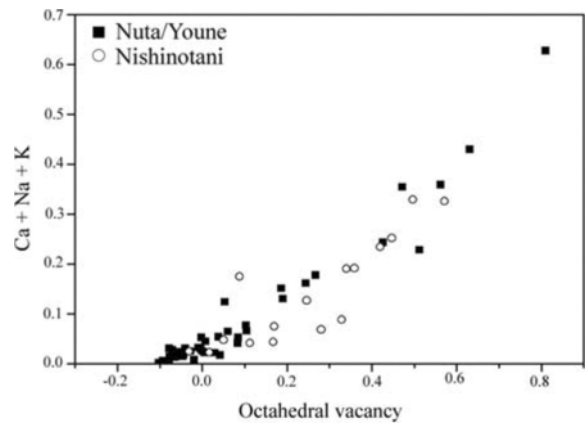

Figure 8. Octahedral vacancy *vs.* (Ca+Na+K) content plots for chlorite. Assuming that all chlorite is trioctahedral, the octahedral vacancy is obtained by Σoct − 12.

https://doi.org/10.1346/CCMN.2005.0530504 Published online by Cambridge University Press

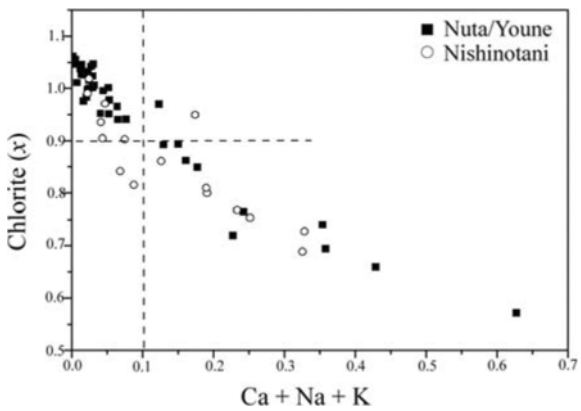

Figure 9. (Ca+Na+K) content *vs*. chlorite ratio (x) plots for chlorite in phenocrysts. The x value is obtained by the Wise method.

1980; Jahren and Aagaard, 1989), which led Cathelineau and Nieva (1985) to apply the concept of tetrahedral Al occupancy as a geothermometer. However, even if impurities such as fine-grained smectite and corrensite are ignored, the chemical composition of chlorite is significantly affected by the presence of smectite layers within the chlorite packets. The chemical composition of chlorite is therefore considered to be unsuitable for use as a geothermometer.

Existence of Fe^{3+}

All Fe was assumed to be Fe^{2+} in the present analysis. This assumption has been adopted in many previous studies on low-grade metamorphic regions. In some chlorites, however, the total number of octahedral

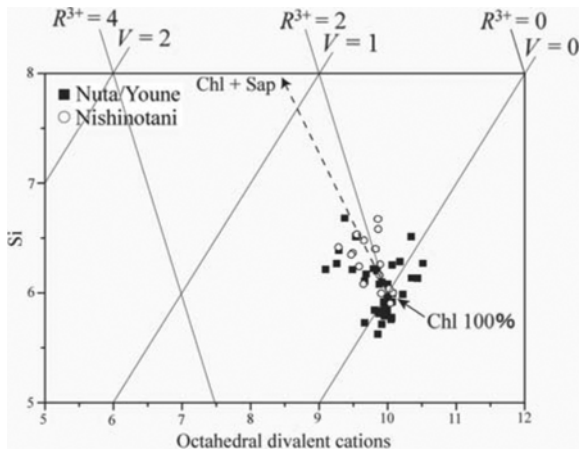

Figure 10. Octahedral divalent cations *vs*. Si plots (after Jiang *et al*., 1994). The dashed lines show schematic trends of mixtures of chlorite (#1Chl: $(Fe^{2+}_{2.77},Mg_{7.23},Mn^{2+}_{0.04},Al_{1.79},\ Cr^{3+}_{0.19})(Si_{5.9},Al_{2.1})O_{20}(OH)_{16}$) with saponite (#2Sap: $Mg_3(Si_{3.67}Al_{0.33})O_{10}(OH)_2$). R^{3+} = octahedral trivalent cations; V = apparent octahedral vacancies. #1 Representative chemical composition from this study, #2 ideal chemical composition. Exchangeable cation and interlayer water are omitted.

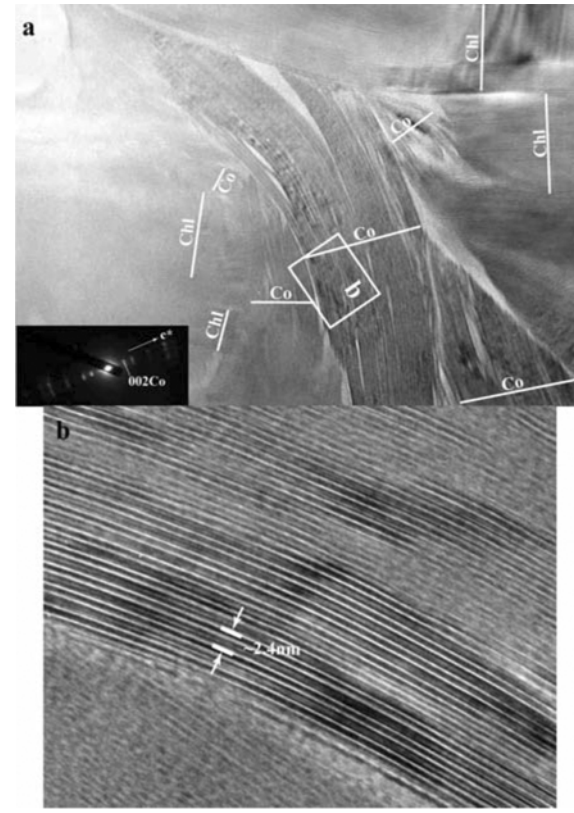

Figure 11. HRTEM images. (a) Lattice fringe image showing corrensite crystallites among chlorite grains. (b) Magnified portion of part a.

cations in a chlorite unit exceeds 12 (Figure 8). Furthermore, as shown in Figure 9, the estimated chlorite ratios for such chlorites are invalid (>100%). It therefore appears that the abundance of Fe^{3+} is underestimated, which may affect the estimated smectite ratio. This suggests that the abundance and influence of Fe^{3+} in chlorite formed in low-grade metamorphic regions should be re-evaluated.

CONCLUSIONS

Through XRD, EMPA and HRTEM analyses, chlorite in metabasites sampled from the Mikabu and North Chichibu belts is identified as a chlorite-smectite mixed-layer mineral. The theoretically estimated smectite ratio is consistent with the smectite ratio determined by observation. The chlorite contains an average of 4% smectite, even in samples exhibiting a (Ca+Na+K) cation content of <0.10 per chlorite unit. The estimated smectite ratio is affected in some cases by the presence of fine-grained interstitial smectite and corrensite as impurities, which are beyond the resolution of EMPA. Such fine-grained smectite and corrensite also contribute to the (Ca+Na+K) content in some chlorites. The present results show that although the Wise method is useful for estimating the proportions of chlorite and smectite in

https://doi.org/10.1346/CCMN.2005.0530504 Published online by Cambridge University Press

chlorite-smectite mixed-layer minerals, HRTEM observations are necessary to qualify the results.

ACKNOWLEDGMENTS

The authors would like to thank Dr J. Ando for assistance with HRTEM observations. Thanks are also extended to H. Ishisako, K. Shibata and Y. Uno for help with XRD, EMPA and HRTEM analyses. Professor R. Yatabe is gratefully acknowledged for providing the cores. The authors thank P. Árkai and R. Klimentidis for constructive reviews of the manuscript. Part of the HRTEM work was supported under the Nanotechnology Support Project of the Ministry of Education, Culture, Sports, Science and Technology (MEXT), Japan.

REFERENCES

Ahn, J.H. and Peacor, D.R. (1985) Transmission electron microscopic study of diagenetic chlorite in Gulf coast argillaceous sediments. *Clays and Clay Minerals*, **33**, 228–236.

Alt, J.C. (1999) Very low-grade hydrothermal metamorphism of basic igneous rocks. Pp. 169–201 in: *Low-grade Metamorphism* (M. Frey and D. Robinson, editors). Blackwell Science Ltd, Oxford, UK.

Árkai, P. and Ghabrial, D.S. (1997) Chlorite crystallinity as an indicator of metamorphic grade of low-temperature metaigneous rocks: a case study from the Bükk Mountains, northeast Hungary. *Clay Minerals*, **32**, 205–222.

Bailey, S.W. (1980) Summary of recommendations of AIPEA nomenclature committee on clay minerals. *American Mineralogist*, **65**, 1–7.

Banno, S. and Sakai, C. (1989) Geology and metamorphic evolution of the Sanbagawa metamorphic belt, Japan. Pp. 519–532 in: *Evolution of Metamorphic Belts* (J.S. Daly, R.A. Cliff and B.W.D. Yardley, editors). Geological Society Special Publication, **43**, Blackwell Scientific Publications, Oxford, UK.

Barrenechea, J.F., Rodas, M., Frey, M., Alonso-Azcárate, J. and Mas, J.R. (2000) Chlorite, corrensite, and chlorite-mica in late Jurassic Fluvio-Lacustrine sediments of the Cameros Basin of Northeastern Spain. *Clays and Clay Minerals*, **48**, 256–265.

Bettison, L.A. and Schiffman, P. (1988) Compositional and structural variations of phyllosilicates from the Point Sal ophiolite, California. *American Mineralogist*, **73**, 62–76.

Bettison-Varga, L., Mackinnon, I.D.R. and Schiffman, P. (1991) Integrated TEM, XRD and electron microprobe investigation of mixed-layer chlorite-smectite from the Point Sal ophiolite, California. *Journal of Metamorphic Geology*, **9**, 697–710.

Bevins, R.E., Robinson, D. and Rowbotham, G. (1991) Compositional variations in mafic phyllosilicates from regional low-grade metabasites and application of the chlorite geothermometer. *Journal of Metamorphic Geology*, **9**, 711–721.

Black, P.M. (1975) Mineralogy of New Caledonian Metamorphic Rocks. *Contributions to Mineralogy and Petrology*, **49**, 269–284.

Buatier, M.D., Früh-Green, G.L. and Karpoff, A.M. (1995) Mechanisms of Mg-phyllosilicate formation in a hydrothermal system at a sedimented ridge (Middle Valley, Juan de Fuca). *Contributions to Mineralogy and Petrology*, **122**, 134–151.

Cathelineau, M. (1988) Cation site occupancy in chlorites and illites as a function of temperature. *Clay Minerals*, **23**, 471–485.

Cathelineau, M. and Nieva, D. (1985) A chlorite solid solution geothermometer The Los Azufres (Mexico) geothermal system. *Contributions to Mineralogy and Petrology*, **91**, 235–244.

Dallmeyer, R.D., Takasu, A. and Yamaguchi, K. (1995) Mesozoic tectonothermal development of the Sanbagawa, Mikabu and Chichibu belts, south-west Japan: evidence from $^{40}Ar/^{39}Ar$ whole-rock phyllite ages. *Journal of Metamorphic Geology*, **13**, 271–286.

Fawcett, J.J. and Yoder, H.S., Jr. (1966) Phase relationships of chlorites in the system MgO-Al_2O_3-SiO_2-H_2O. *American Mineralogist*, **51**, 353–380.

Foster, M.D. (1962) Interpretation of the composition and a classification of the chlorites. U.S. Geological Survey Professional Paper, **414-A**. US Government Printing Office, Washington, D.C., 26 pp.

Guthrie, G.D., Jr. and Veblen, D.R. (1990) Interpreting one-dimensional high-resolution transmission electron micrographs of sheet silicates by computer simulation. *American Mineralogist*, **75**, 276–288.

Hillier, S. and Velde, B. (1991) Octahedral occupancy and the chemical composition of diagenetic (low-temperature) chlorites. *Clay Minerals*, **26**, 149–168.

Inoue, A. and Utada, M. (1991) Smectite-to-chlorite transformation in thermally metamorphosed volcanoclastic rocks in the Kamikita area, northern Honshu, Japan. *American Mineralogist*, **76**, 628–640.

Isozaki, Y. and Itaya, T. (1990) K-Ar ages of weakly metamorphosed rocks at the northern margin of Kurosegawa Terrane in central Shikoku and western Kii Peninsula – extent of the Kurosegawa Terrane in Southwest Japan. *Journal of the Geological Society of Japan*, **96**, 623–639 (in Japanese with English abstract).

Isozaki, Y., Maruyama, S. and Furuoka, F. (1990) Accreted oceanic materials in Japan. *Tectonophysics*, **181**, 179–205.

Jahren, J.S. and Aagaard, P. (1989) Compositional variations in diagenetic chlorites and illites, and relationships with formation-water chemistry. *Clay Minerals*, **24**, 157–170.

James, R.S., Turnock, A.C. and Fawcett, J.J. (1976) The stability and phase relations of iron chlorite below 8.5 kb P_{H_2O}. *Contributions to Mineralogy and Petrology*, **56**, 1–25.

Jiang, W.-T. and Peacor, D.R. (1991) Transmission electron microscopic study of the kaolinitization of muscovite. *Clays and Clay Minerals*, **39**, 1–13.

Jiang, W.-T., Peacor, D.R. and Slack, J.F. (1992) Microstructures, mixed layering, and polymorphism of chlorite and retrograde berthierine in the Kidd creek massive sulfide deposit, Ontario. *Clays and Clay Minerals*, **40**, 501–514.

Jiang, W.-T., Peacor, D.R. and Buseck, P.R. (1994) Chlorite geothermometry? Contamination and apparent octahedral vacancies. *Clays and Clay Minerals*, **42**, 593–605.

Kashima, N. (1969) Stratigraphical Studies of the Chichibu Belt in Western Shikoku. *Memoirs of the Faculty of Science, Kyushu University, Series D Geology*, **19**, 387–436.

Kawato, K., Isozaki, Y. and Itaya, T. (1991) Geotectonic boundary between the Sanbagawa and Chichibu belts in central Shikoku, Southwest Japan. *Journal of the Geological Society of Japan*, **97**, 959–975 (in Japanese with English abstract).

Klimentidis, R.E. and Mackinnon, I.D.R. (1986) High-resolution imaging of ordered mixed-layer clays. *Clays and Clay Minerals*, **34**, 155–164.

López-Munguira, A., Nieto, F. and Morata, D. (2002) Chlorite compositions and geothermometry: a comparative HRTEM/AEM-EMPA-XRD study of Cambrian basic lavas from the Ossa Morena Zone, SW Spain. *Clay Minerals*, **37**, 267–281.

Martínez-Serrano, R.G. and Dubois, M. (1998) Chemical variations in chlorite at the Los Humeros geothermal system, Mexico. *Clay Minerals*, **46**, 615–628.

Maruyama, S. and Liou, J.G. (1985) The stability of Ca-Na pyroxene in low-grade metabasites of high-pressure intermediate facies series. *American Mineralogist*, **70**, 16–29.

Mata, M.P., Giorgetti, G., Árkai, P. and Peacor, D.R. (2001) Comparison of evolution of trioctahedral chlorite/berthierine/smectite in coeval metabasites and metapelites from diagenetic to epizonal grades. *Clays and Clay Minerals*, **49**, 318–332.

Matsuoka, A. (1985) Middle Jurassic Keta Formation of the southern part of the Middle Chichibu Terrane in the Sakawa area, Kochi Prefecture, Southwest Japan. *Journal of the Geological Society of Japan*, **91**, 411–420.

McDowell, S.D. and Elders, W.A. (1980) Authigenic layer silicate minerals in Borehole Elmore 1, Salton Sea Geothermal Field, California, USA. *Contributions to Mineralogy and Petrology*, **74**, 293–310.

Miyahara, M. (2004) Genesis and mineralogical study on chlorite in metabasites in the Mikabu belt and the North-Chichibu belt, Shikoku Island, SW Japan. PhD thesis, University of Hiroshima, Hiroshima, Japan, 113 pp.

Miyahara, M. and Ishisako, H. (2004) The simple preparation technique of a fragile specimen for HRTEM observation. *Clay Science*, **12**, 271–275.

Moore, D.M. and Reynolds, R.C., Jr. (1997) *X-ray Diffraction and the Identification and Analysis of Clay Minerals*. Oxford University Press, New York, 378 pp.

Morikiyo, T. (1979) Petrological study on the Mikabu green rocks from Kenzan district, Tokushima Prefecture. *Journal of the Geological Society of Japan*, **85**, 299–306 (in Japanese with English abstract).

Murata, A. (1982) Large Decke Structures and their formative process in the Sambagawa-Chichibu, Kurosegawa and Sambosan terrains, Southwest Japan. *Journal of the Faculty of Science, University of Tokyo, Section 2, Geology, Mineralogy, Geography, Geophysics*, **20**, 383–424.

Ozawa, H., Motoyama, S., Inoue, S., Kato, Y. and Murata, M. (1999) Petrology of basic volcanics of the Mikabu greenstone complex in the eastern Shikoku. *The Memoirs of the Geological Society of Japan*, **52**, 217–228 (in Japanese with English abstract).

Schiffman, P. and Fridleifsson, G.O. (1991) The smectite-chlorite transition in drillhole Nj-15, Nesjavellir geothermal field, Iceland: XRD, BSE and electron microprobe investigations. *Journal of Metamorphic Geology*, **9**, 679–696.

Schmidt, D., Livi, K.J.T. and Frey, M. (1999) Reaction progress in chloritic material: an electron microbeam study of the Taveyanne greywacke, Switzerland. *Journal of Metamorphic Geology*, **17**, 229–241.

Sharp, T.G. and Buseck, P.R. (1988) Prograde versus retrograde chlorite-amphibole intergrowths in a calc-silicate rock. *American Mineralogist*, **73**, 1292–1301.

Shau, Y.-H. and Peacor, D.R. (1992) Phyllosilicates in hydrothermally altered basalts from DSDP Hole 504B, Leg83 – a TEM and AEM study. *Contributions to Mineralogy and Petrology*, **112**, 119–133.

Suyari, K., Kuwano, Y. and Ishida, K. (1980) Stratigraphy and geological structure of the Mikabu Greenrock Terrain and its environs – I The Tosa-cho and Motoyama-cho Areas, central Kochi Prefecture. *Journal of Science, University of Tokushima*, **8**, 63–82 (in Japanese with English abstract).

Suyari, K., Kuwano, Y. and Ishida, K. (1982) Stratigraphy and geological structure of the Mikabu Greenrock Terrain and its environs – II Some information about the Mesozoic stratigraphy of the North Sub-belt of the Chichibu Belt. *Journal of Science, University of Tokushima*, **15**, 51–71 (in Japanese with English abstract).

Suzuki, T. (1972) Volcanism and metamorphism of the Mikabu Green-Rocks in Central and Western Shikoku. *Research reports of Kochi University, Natural Science*, **21**, 39–62 (in Japanese with English abstract).

Suzuki, S. and Ishizuka, H. (1998) Low-grade metamorphism of the Mikabu and northern Chichibu belts in central Shikoku, SW Japan: implications for the areal extent of the Sanbagawa low-grade metamorphism. *Journal of Metamorphic Geology*, **16**, 107–116.

Takeda, K. (1984) Geological and petrological studies of the Mikabu Greenstones in Eastern Shikoku, southwest Japan. *Journal of Science of Hiroshima University, Series C*, **8**, 221–282.

Xie, X., Byerly, G.R. and Ferrell, R.E., Jr. (1997) IIb trioctahedral chlorite from the Barberton greenstone belt: crystal structure and rock composition constraints with implications to geothermometry. *Contributions to Mineralogy and Petrology*, **126**, 275–291.

Zane, A., Sassi, R. and Guidotti, C.V. (1998) New data on metamorphic chlorite as a petrogenetic indicator mineral, with special regard to greenschist-facies rocks. *The Canadian Mineralogist*, **36**, 713–726.

(*Received 1 August 2005; revised 9 April 2005; Ms. 944; A.E. Warren D. Huff*)